



Seismic Damage Accumulation in Reinforced Concrete Structures due to Mainshock and Aftershock

K. Duerr and S. Tesfamariam

Okanagan School of Engineering, The University of British Columbia, 3333 University way, Kelowna, BC, Canada, V1V 1V7

Abstract: Anticipating structure seismic performance is important in moderate to high seismic hazard regions. Knowledge of probable earthquake locations and strengths are used to determine the possible consequences to a structure based on performance. One area of performance-based earthquake engineering (PBEE) that is relatively underdeveloped is the incorporation of aftershocks for calculating the performance of a structure. In 2011, the earthquakes of Japan and New Zealand have shown aftershocks can be of significant strength and impact. In this paper, the impact of mainshocks and aftershocks on the damage accumulation of a reinforced concrete (RC) structure is investigated. Different return period seismic hazards are generated from past earthquake event records to accurately test the structure's performance. A seven story RC structure is modeled in OpenSees software and subject to mainshocks and aftershocks based on the seismic hazard. The analysis method of OpenSees allows the structure behavior to be measured continuously throughout the simulation. A selection of damage indices are used to quantify the damage of the structure based on the behavior. The damage accumulation that occurs during sequential mainshock and aftershock events is presented. The impact of aftershock events on structural performance is discussed.

1. Introduction

The goal of the seismic analysis is often to anticipate the real-world response of the structure and is core concept of performance-based earthquake engineering (PBEE). Mainshock is often the focus of the seismic hazard analysis for a structure but it is increasingly apparent that consideration of aftershocks is important. For example, in Christchurch, New Zealand earthquake, the September 2010 M_w 7.2 mainshock was followed by the February 2011 M_w 6.2 aftershock. The weaker aftershock event has caused a significant amount of damage and loss of life; more so than the associated mainshock (Reyners 2011). The March 2011 earthquakes in Japan also had significant foreshock and aftershock events (Satoshi et al. 2011). While the mainshock event in Japan was certainly one of the strongest in recent history, the foreshocks and aftershocks of this event are significant events even when considered individually. These examples highlight the impact of aftershock events when included with the mainshock.

Bazzurro et al. (2004) presented a method to estimate the damage level of a structure after an aftershock to assist with the post-earthquake damage assessment and inspection that typically occurs. It is important to know the risk due to aftershocks because that can affect what occupancy is set for that structure after a mainshock occurs. Yeo and Cornell (2005) produced a PEER report on the stochastic characterization and time-dependent aftershock risk for PBEE. With the method provided in the report, Yeo and Cornell performed a life-cycle analysis based on

different aftershock models. Li and Ellingwood (2007) investigated the damage to a steel moment frame due to mainshock-aftershock sequences. A result of the work was showing that mainshock-aftershock sequences caused significantly more damage than mainshocks alone. An important consideration presented by Li and Ellingwood (2007) is that damage assessment modeling can be reasonably represented with a single aftershock event. Jalayer et al. (2010) presented a Bayesian updating framework for improving the hazard analysis of mainshocks and aftershocks as new data became available. From the works mentioned in this section, it is clear that aftershocks are an important part of seismic hazard analysis.

Along with applying appropriate hazard in PBEE, appropriate response parameters should be evaluated. Inter-story drift (ISD) is a common performance measurement for seismic response analysis. ISD is often used because it is easy to measure or calculate and there are established guidelines for acceptable limits on ISD (Ghobarah 2001, FEMA 356). A downside of ISD is that information about the local behaviour of structural elements is lost. Without the local behaviour, it can be difficult to identify the critical elements in a structure. One method to identify local behaviour is to use damage indices (e.g. Ghobarah 2000). Damage indices are a class of methods that relate different response parameters, such as deflection, stress, or others, to the capacity. Value of the damage index varies from zero to one representing, respectively, undamaged and collapse limit states. With the local response represented by a damage index, the structural elements critical to the seismic performance can be identified and building damage quantified (Williams and Sexsmith 1995). Decisions can then be made to address any deficiencies in the critical members and to improve the overall seismic performance of the structure.

With the consideration of mainshock and aftershocks, it is beneficial to see the accumulation of damage in the structure as opposed to only the final damage level. Applying damage accumulation analysis on a global level can show how the damage progresses in the different sections of the structure and how the load paths will change as members fail. Damage accumulation can also relate damage level to specific points of time during the earthquake; the most damaging portions of an earthquake can be identified and, in the case of multiple seismic events, the damage contribution of different events can be determined. Thus, this paper presents an investigation into the effect of mainshock-aftershocks sequences on damage accumulation using damage indices. In the following sections, the selection of site seismic hazard and damage indices will be discussed. Finally, the proposed method will be highlighted with a 7 storey reinforced concrete (RC) building, and the ensuing damage accumulation results will be discussed.

2. Seismic Hazard

There are many factors that influence the seismic hazard for a given structure. Site location is generally the most important factor as it includes fault proximity, fault type, soil conditions. If a specific site location is known then the site specific factors can be determined and a representative seismic hazard can be calculated. With enough historical data for a region a typical seismic event record can also be used. If the typical event is not known or if more general analysis is required then a set of earthquake records can be used to represent the variety of earthquake possibilities. Such a record set can be obtained by selecting natural earthquake records from historical events around the world. FEMA P695 (2009) has provided a robust set of natural earthquake records from the PEER NGA ground motion database. The record set is representative of a wide range of possible site hazards and is not specific to a location.

Ground motion records can be scaled to meet a given hazard level. There are generally two ways to scale the ground motion record to the UHS. The first method is commonly used as it is quick and easy to apply. The UHS is compared to the spectral period content of the ground motion record. At the value of the structure's natural period, the ground motion intensity is scaled by a factor that matches the ground motion spectrum to the UHS. This method is to ensure the ground

motion applied to the test structure is the same intensity as an earthquake the structure would be expected to experience. The second method again compares the ground motion spectral period content to that of the UHS but instead applies a method presented by Abrahamson (1992) and Hancock et al. (2006). This method generates wavelets to modify the earthquake record to more closely match the UHS. Compared to the first method, the second method does not provide as accurate matching at the specific structure period but does include a wider range of periods in the matching.

3. Damage Indices

The damage indices attempt to describe the behaviour for the structural element. The specific mechanisms that the damage indices are based on vary but most involve the hysteretic stress-strain behaviour of the structural member. There are many damage indices available but for the purposes of this paper Park and Ang (Park et al. 1984) and Kratzig (Kratzig et al. 1989), a small selection will be discussed. The damage indices presented in this section were chosen to represent commonly used methods. These damage indices include both deformation, and energy based methodologies.

3.1 Park and Ang

The Park and Ang damage index D (Park et al. 1984) was developed as a hybrid method, which includes both displacement and dissipated hysteretic energy. This is a commonly used damage quantification method and can be computed using Equation 1.

$$[1] \quad D_{PA} = \frac{\delta_m}{\delta_u} + \beta_e \frac{\int dE}{F_y \delta_u}$$

where, δ_m = maximum deformation response to the excitation; δ_u = ultimate deformation capacity under monotonic loading; F_y = element yield strength; β_e = non-negative calibration parameter; dE = incremental dissipated hysteretic energy.

The first term measures the displacement based damage where the maximum displacement δ_m is compared to its ultimate displacement δ_u . The second term uses the dissipated energy of the element to account for the accumulated damage and it is compared to the ultimate energy capacity to measure failure. A range of values for β_e have been presented and it has been shown that the calibration factor has a significant impact on the accuracy of the damage index. The generally recommended range for the calibration factor is between 0.1 and 0.5 (Williams and Sexsmith 1995). In subsequent work, this method has been expanded upon to use moment and rotation instead of force and deflection as the basis for the damage but in this work the original method is used.

The resultant value of D represents the approximate damage level to the structural element. The initially proposed classification of the damage index values as compared to the actual damage level is presented in Table 1. Later research by Park and Ang has recommended the damage index value for the collapsed state should be reduced to 0.8 from 1.0.

Table 1: Classification of Park and Ang damage Index (Williams and Sexsmith 1995)

Damage index value	Structure damage level
$D < 0.1$	No damage or minor cracking
$0.1 \leq D < 0.25$	Minor damage – light cracking throughout
$0.25 \leq D < 0.4$	Moderate damage – Severe cracking, localized spalling
$0.4 \leq D < 1$	Severe damage – Crushing of concrete, reinforcement exposed
$D \geq 1$	Collapsed

3.2 Kratzig

Kratzig et al. (1989) presented a formulation using the energy dissipation of the structural members. The method is based on the definition of primary and follower half-cycles shown in Figure 1. A primary half-cycle (PHC) is defined as the first half cycle of loading at a given amplitude. Subsequent half-cycles are follower half-cycles (FHC) unless they exceed the previous maximum amplitude. For positive element deformation, the positive damage parameter is (Kratzig et al. 1989):

$$[2] \quad D_k^+ = \frac{\sum E_{p,i}^+ + \sum E_i^+}{E_f^+ + \sum E_i^+}$$

where $E_{p,i}$ = the energy in a PHC; E_i = the energy in a FHC; E_f = the energy absorbed by the element in a test to failure.

Equation 2 can be used for a similar parameter for the negative displacement case. The positive and negative parameters are combined for the overall damage index as shown in Equation 3.

$$[3] \quad D_k = D_k^+ + D_k^- - D_k^+ D_k^-$$

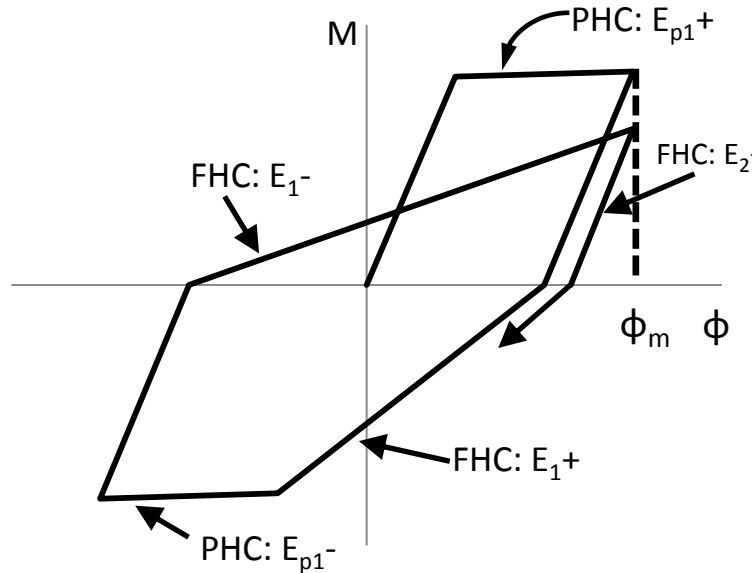


Figure 1: Primary (PHC) and follower (FHC) half cycles (Kratzig *et al.*, 1989)

This method accounts for the energy dissipated by a structural member and thus includes the force and displacement experienced by that member. In summary, the energy of the strongest cycles is compared to the energy capacity at failure while the energy from other cycles is included to account for the continuous accumulated energy dissipation. The combination of PHC and FHC energy has been shown to approach unity at failure (Williams and Sexsmith 1995).

To aggregate the index values for a set of structural elements, a formula was suggested by Williams and Sexsmith (1995) based on previous methods. This formula is shown in Equation 4. This equation places the emphasis on higher damage index values.

$$[4] \quad D_{set} = \frac{D_i^2}{D_i}$$

4. Illustrative Example

The damage accumulation will be illustrated with a RC building reported in Krawinkler (2005). This structure is a seven story hotel built in Van Nuys, California, USA (Figure 2). This building was constructed in 1965 according to the 1964 Los Angeles City Building Code. The building is 7 storeys, 8 bays by 3 bays, RC moment resisting frame. The report included many of the design and material properties of the building such as reinforcement detailing and concrete strength. This building is useful because it represented current practise at the time of construction and is seismically deficient according to current design codes.

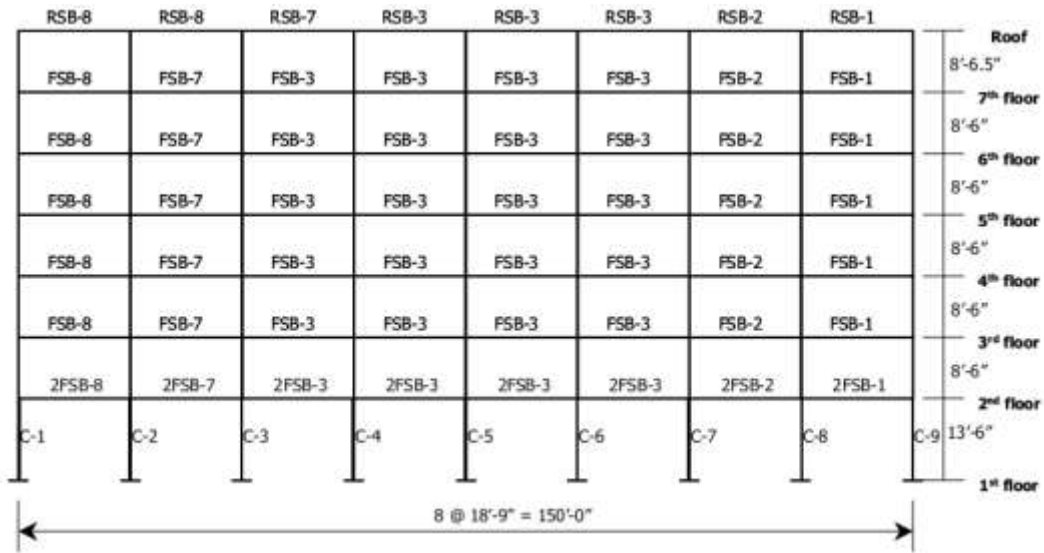


Figure 2: South frame elevation of Van Nuys Hotel (adapted from Krawinkler 2005).

The simulation of the Van Nuys hotel was completed in the OpenSees software platform. This open source software is supported by the Pacific Earthquake Engineering Research Center (PEER) and the George E. Brown, Jr. Network for Earthquake Engineering Simulation (NEES) and is designed specifically to model a structure's performance during an earthquake and provide meaningful results. The hotel building was modeled in the Opensees software based on the reinforcement detailing provided by Krawinkler (2005). The structural elements were modeled within OpenSees as lumped plasticity elements.

The ground motion records applied to the structure model were based on the FEMA P695 record set and scaled to the USGS UHS for California using SeismoMatch software¹. To illustrate the hazard level of 10%/50 years for the mainshock, representing a rare 475 year event, and 15%/50 years for the aftershock were chosen to illustrate the damage progression in the test structure. This lower hazard level was selected due to vulnerability of the test structure, as a higher intensity would collapse the structure. A plot of the scaled mainshock and aftershock spectra with the respective target UHS is shown in Figure 3.

¹ <http://www.seismosoft.com>

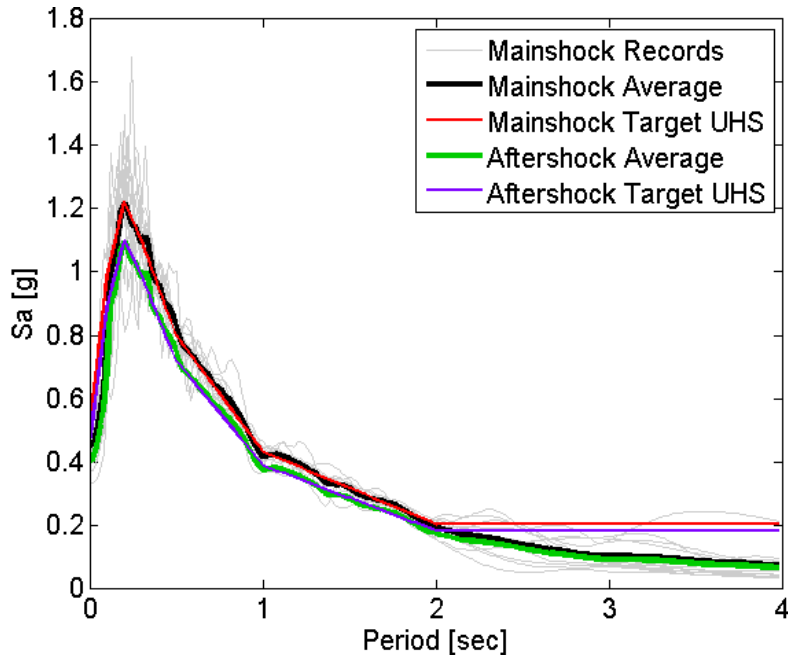


Figure 3: 10%/50 years for the mainshock and 15%/50 year aftershock seismic hazard

5. Results

The simulations were run with a set of FEMA P695 records scaled to the USGS UHS for California of 10%/50 years for the mainshocks and 15%/50 years for the aftershocks. As the test structure is non-code conforming and the seismic hazard for the California region is high, the simulations resulted in varying levels of damage. Between the between the mainshock and aftershock events a delay was placed to allow the building to reduce its motion and separate the effect of the two events.

From the OpenSees simulation analysis, a number of different types of data can be recorded. The inter-story drift and damage index values were computed for all of the mainshock and aftershock simulations. Figure 4 shows an example of the ISD values taken from a simulation. In this figure, one can clearly see some important parts of the simulation. The initial mainshock event, the following aftershock event, the intervening delay, and time periods of increased damage are all apparent. All of the seismic record simulations are similar to Figure 4 in that the periods of high ISD are correlated with the shifts in residual ISD.

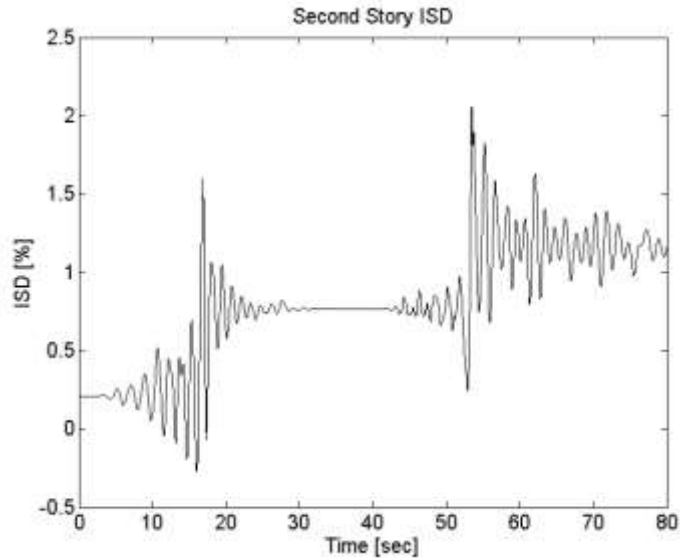


Figure 4: Example time history of a second story drift ratio for a structure subject to mainshock and aftershock

Average value of the resulting ISD for all simulations results is shown in Figure 5. Both the residual and maximum ISD is increased due to the aftershock event. The third storey shows the highest drift value.

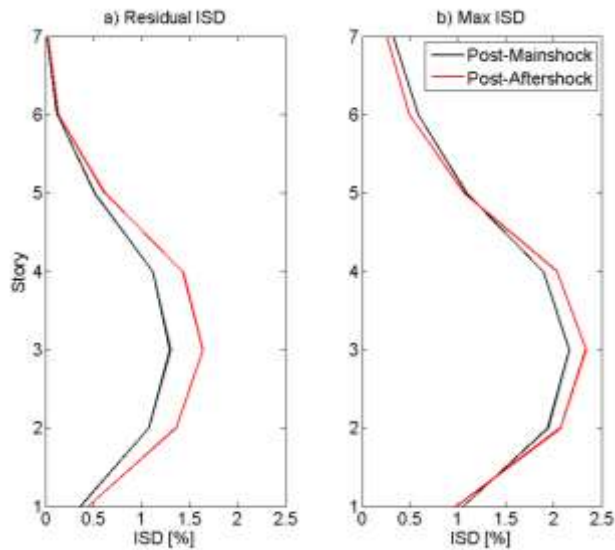


Figure 5: Post-mainshock and -aftershock for a) Residual ISD, b) Maximum ISD, averaged for all seismic records

The hysteretic response of each ground motion is used to compute the corresponding individual structural members damage index values for D_{PA} (Equation 1) and D_K (Equation 2). Figures 6a and 6b show the progression of both damage index values with time for D_{PA} and D_K , respectively, given for a single structural element. The different damage value progressions are given for each ground motion. The maximum increase in the damage index values for both indices are associated with the peak values of the scaled ground motions. To show the variability in the results provided by the different ground motions, the damage index values presented in Figure 6a and 6b were fit to a normal distribution. The parameters of the normal distributions for the two damage indices at points before and after the aftershock are shown in Table 2. The mean value of the distribution of D_{PA} and D_K increases by 33% and 21%, respectively.

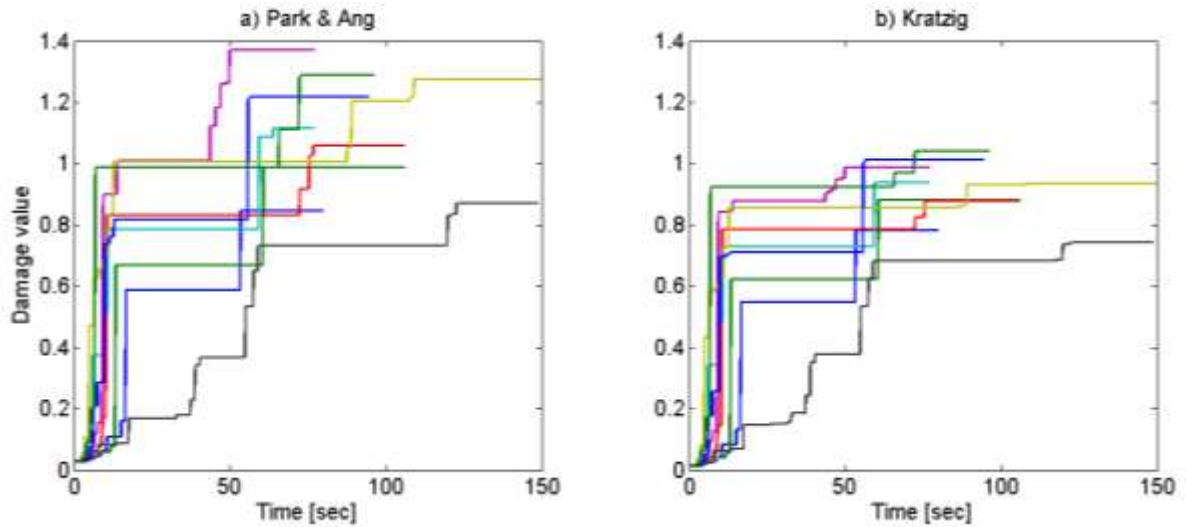


Figure 6: Example progression of damage index values for a) Park and Ang and b) Kratzig damage indices

Table 2: Damage index value distribution parameters for the plots in Figure 6

$N(\mu, \sigma)$	Park & Ang D_{PA}	Kratzig D_K
Pre-Aftershock	$N(0.84, 0.17)$	$N(0.76, 0.15)$
Post-Aftershock	$N(1.12, 0.21)$	$N(0.92, 0.12)$

Using Equation 4, a weighted average of the damage index for the whole structure is calculated. Table 3 summarizes the weighted average values for the D_{PA} and D_K indices. The values before and after the aftershock event are also shown. The average value of D_{PA} and D_K increases by 92% and 24%.

Table 3: Damage index values averaged over the whole structure

	Park & Ang D_{PA}	Kratzig D_K
Pre-Aftershock	0.280	0.409
Post-Aftershock	0.510	0.508

Along with the average damage level for the structure it is also interesting to see the number of structural members that, according to the damage indices, have reached a point of failure. Table 4 shows the number of failed elements averaged over the different record simulations. Again, the values are shown for the two damage indices and for pre- and post-aftershock. Overall, for the higher damage index ($DI > 0.8$), the D_K index showed more sensitivity.

Table 4: Average number of element damage indices indicating failure ($DI > 0.8$)

	Park & Ang D_{PA}	Kratzig D_K
Pre-Aftershock	1.2	1.9
Post-Aftershock	2.9	5.6

6. Discussion and Conclusion

In this paper, the results of a series of simulations show the effect of aftershocks on the damage level of a structure. In general, the aftershocks caused damage beyond the level of the mainshocks. Some mainshock-aftershock combinations did not result in damage much greater than the mainshock alone, but other combinations of event resulted in significant additional damage. All of the seismic records were scaled to the same hazard level thus the difference in damage was not entirely dependent on the earthquake intensity. Other factors, such as overall duration and peak intensity may be responsible.

When considering the performance of the structure, it is clear that the aftershocks cause an increase in damage. The test structure applied in this paper does not conform to current code and is generally lacking in both lateral strength and ductility. Due to limited resources, it may not be feasible to retrofit the structure to a high performance level for mainshock-aftershock sequences; thus this sequence can be used to delineate and optimize the critical sections for retrofitting.

Modern structures built with PBEE in mind are generally designed to be able to withstand a strong event and even be in a repairable state for less significant events. It is less likely that the structure would need to be demolished after a mainshock event. For these modern structures, aftershock analysis becomes more important as one would need to know the potential performance of the structure beyond the mainshock. Damage indices are also useful in PBEE analysis as it provides an additional method to measure the performance of local structural members and the structure as a whole.

Acknowledgement

The financial support from Natural Sciences and Engineering Research Council of Canada (NSERC) under Discovery Grant Program is greatly acknowledged. Additional support is also acknowledged from Mr. Yu Kang of West Edge Engineering and MITACS accelerate program. Thanks to Dr. Haukass Dr. Koduru for sharing OpenSees software with working damage index commands.

References

- Abrahamson, N.A. 1992. Non-stationary spectral matching. *Seismological Research Letters*, 63(1):30.
- Bazzurro, P., Cornell, C.A., Menun, C., and Motahari, M. 2004. Guidelines for Seismic Assessment of Damaged Buildings. *13th World Conference on Earthquake Engineering*. Paper No. 1708.
- FEMA P695. 2009. *Quantification of Building Seismic Performance Factors*. Prepared by ATC for the Federal Emergency Management Agency, Washington, D.C., USA.

- FEMA 356. 2000. *Prestandard and Commentary for the Seismic Rehabilitation of Buildings*. Prepared by ASCE for Federal Emergency Management Agency, Washington, D.C., USA.
- Ghobarah, A. 2001. Performance-based design in earthquake engineering: state of development. *Engineering Structures*, 23:878-884.
- Ghobarah, A. 2000. Seismic Assessment of Existing RC Structures. *Progress in Structural Engineering and Materials*, 2:60-71.
- Hancock J., Watson-Lamprey J., Abrahamson N.A., Bommer J.J., Markatis A., McCoy E., and Mendis R. 2006. An Improved Method of Matching Response Spectra of Recorded Earthquake Ground Motion using Wavelets. *Journal of Earthquake Engineering*, 10:67–89.
- Ide, S., Baltay, A., and Beroza, G.C. 2011. Shallow Dynamic Overshoot and Energetic Deep Rupture in the 2011 M_w 9.0 Tohoku-Oki Earthquake. *Science*, 332 (6036):1426-1429.
- Jaylayer, F., Asprone, D., and Prota, A. 2010. A Decision Support System for Post-earthquake Reliability Assessment of Structures Subjected to Aftershocks: An Application to L'Aquila Earthquake, 2009. *Bulletin of Earthquake Engineering*. 9(4):997-1014.
- Kratzig, W.B., Meyer, I.F., and Meskouris, K. 1989. Damage Evolution in Reinforced Concrete Members under Cyclic Loading. *Proceedings of 5th International Conference on Structural Safety and Reliability (ICOSSAR 89)*, San Francisco CA, Vol. II:795-802.
- Krawinkler, H. 2005. *Van Nuys Hotel Building Testbed Report: Exercising Seismic Performance Assessment*. Pacific Earthquake Engineering Research Center Report 2005/11.
- Li, Q. and Ellingwood, R. 2007. Performance Evaluation and damage assessment of steel frame buildings under main shock-aftershock earthquake sequences. *Earthquake Engineering Structural Dynamics*. 36(3):405-427.
- Park Y.J., Ang A.H-S., and Wen Y.K. 1984. Seismic Damage Analysis and Damage-Limiting Design of R.C. Buildings. *Structural Research Serial Report no UILU-ENG-84-2007*, University of Illinois at Urbana-Champaign, Urbana, IL.
- Reyners, M. 2011. Lessons from the destructive Mw 6.3 Christchurch, New Zealand, Earthquake. *Seismological Research Letters*, 82(3):371-372
- Williams, M.S. and Sexsmith, R.G. 1995. Seismic Damage Indices for Concrete Structures: A State-of-the-Art Review. *Earthquake Spectra*, 11:319-349.
- Yeo, G.L. and Cornell, C.A. 2005. *Stochastic Characterization and Decision Bases under Time-Dependent Aftershock Risk in Performance-Based Earthquake Engineering*. Pacific Earthquake Engineering Research Center Report, July, 2005. Stanford University Department of Civil and Environmental Engineering.